Chapter 5
1D TiO_2 Nanotube-Based Photocatalysts

Fang-Xing Xiao and Bin Liu

Abstract In this chapter, the latest developments of one-dimensional semiconductors, typically TiO_2 nanotube arrays (TNTAs) in the photocatalysis, are reviewed including the modification strategies for preparing TNTA-based photocatalysts, diverse photocatalytic applications of TNTA-based hybrid nanostructures in a myriad of fields, and a perspective on future challenges regarding the design and improvement of TNTAs for photocatalysis.

Keywords One dimensional • TiO_2 nanotube arrays • Photocatalysis • Photoelectrochemical

5.1 Introduction

In recent years, sustainable developments of human being are retarded by increasingly serious environmental pollution and depletion of fossil fuel resources [1]. To surmount these obstacles, various technologies have been extensively developed to reduce the environmental and energy crisis by conventional techniques including adsorption, precipitation, and osmosis [2]. Although intense endeavors have been made to impede the deterioration of these two crises, it is still challenging to develop an efficient and green technique to control and reduce the pollution growth. Photocatalysis, as a novel route to achieve deep mineralization of organic pollutants toward carbon dioxide and water under light irradiation, has attracted enormous attention on account of its great efficiency and promising potential applications [3]. Among various semiconductors, TiO_2 has been determined as the most widely used photocatalyst for versatile photocatalytic applications such as hydrogen production, CO_2 reduction, selective organic transformation, and nonselective organic oxidation, owing to its environmental friendliness, stable chemical and physical properties, nontoxicity, and durability [4, 5].

Up to date, a large variety of TiO_2 nanostructures have been prepared for photocatalytic investigations which mainly include nanoparticles, nanowires,

F.-X. Xiao • B. Liu (✉)
School of Chemical and Biomedical Engineering, Nanyang Technological University, 62 Nanyang Drive, Singapore 637459, Singapore
e-mail: liubin@ntu.edu.sg

J.C. Colmenares, Y.-J. Xu (eds.), *Heterogeneous Photocatalysis*, Green Chemistry and Sustainable Technology, DOI 10.1007/978-3-662-48719-8_5

nanorods, nanosheets, and nanotubes [6]. Among which, TiO_2 nanotube arrays (TNTAs) growing vertically from Ti foil afforded by electrochemical anodization can serve as an ideal platform for exploring new photocatalysts [7]. The structural advantages of TNTAs predominantly center on the following several aspects. Firstly, one-dimensional geometry of TNTAs with smooth surface is beneficial for efficient charge transfer, thus providing significantly shorter carrier-diffusion paths along the tube walls and minimizing the charge losses arising from electron hopping between nanoparticles in comparison with corresponding bulk TiO_2 nanoparticles [8]. Secondly, owing to direct growth property of TNTAs on Ti substrate, it is convenient to separate the TNTA-based photocatalysts from reaction systems for recycling reactions, thus reducing tedious recovery procedures for practical applications [9]. Despite the developments of TNTAs in the field of heterogeneous photocatalysis during the past few years, two intrinsic drawbacks still remarkably retard their potential applications. Specifically, wide bandgap of TNTAs (i.e., 3.2 eV) requires UV light irradiation to trigger the photocatalytic reactions, which accounts for only a small fraction of (ca. 5 %) solar spectrum in comparison with visible light (52 %) and infrared light (43 %). Additionally, fast recombination of photogenerated electron–hole charge carriers over TNTAs substantially reduces the efficiency of photocatalytic reactions. In this regard, it is highly desirable to shift the optical response of TNTAs toward visible or even infrared region in conjunction with high separation efficiency of photoexcited charge carriers for boosting the photocatalytic performances of TNTA-based photocatalysts. To this end, various strategies have therefore been developed to conquer the disadvantage of TNTAs including metal or nonmetal element doping [10, 11], noble metal deposition [12], sensitization with narrow-bandgap semiconductors [13], and formation of p–n heterojunction [14], just named a few, which will be specifically elucidated in the following parts.

In this chapter, we primarily focus on the state-of-the-art developments of TiO_2 nanotube with an emphasis on the TNTA-based nanocomposites, the content of which primarily contains basic introduction of TNTAs, preparation of varieties of TNTA-based heterostructures, and their diverse photocatalytic applications in a myriad of fields. Finally, a perspective on future challenges regarding the design and improvement of TNTAs for photocatalysis is afforded. It is hoped that this chapter could provide enriched information on the potential applications of TiO_2 nanotube-based nanocomposites as multifunctional photocatalysts.

5.2 Basic Introduction of TNTAs

The fabrication of TNTAs via anodic oxidation of titanium foil in a fluoride-based solution was firstly reported in 2001 by Grimes and co-workers [15]. Since then, precise control over the nanotube morphology, length, pore size, and wall thickness has been the focus of many studies [16, 17]. It has been well established that electrolyte composition plays an imperative role in determining the architecture

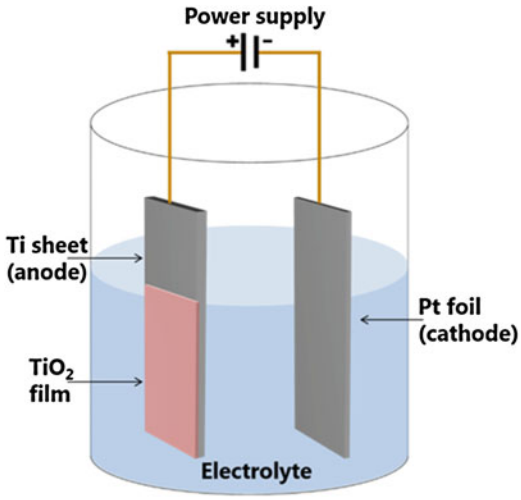

Scheme 5.1 Experimental setup for preparing the TNTAs

and chemical composition of nanotube arrays. In particular, the formation rate of TNTAs can be tuned by electrolyte composition and its pH value.

The key process responsible for anodic preparation of TNTAs mainly includes the following four processes: (1) oxide growth on the metal surface owing to the interaction of metal with O^{2-} or OH^- ions. The in situ formed anions during the formation of an initial oxide layer can migrate through the oxide layer approaching the metal/oxide interface where they react with the metal [18]. (2) Ti^{4+} migrated from the metal at the interface will be rapidly released under an exerted external electric field and move toward the oxide/electrolyte interface. (3) The third process is the field-assisted dissolution of the oxide at the oxide/electrolyte interface [19]. The Ti–O bond is weakened under applied electric field giving rise to dissolution of the Ti^{4+} which dissolves into the electrolyte and interacts with the free O^{2-} anions at the interface [20, 21]. (4) Chemical dissolution of titania in the HF electrolyte also takes place during the anodization process. Based on the above mechanism, highly ordered and self-aligned TNTAs were thus prepared. The experimental setup for preparing TNTAs was illustrated in Scheme 5.1.

5.3 TNTA-Based Photocatalysts

5.3.1 TNTAs with Nonmetal Element Doping

Vertically oriented TNTAs have been regarded as an ideal candidate for photocatalytic applications, such as water splitting to produce H_2 and photocatalytic degradation of organic dye pollutants, owing to their high catalyst/electrolyte interface area, electrolyte percolation, and remarkably enhanced

separation of photogenerated electron–hole charged careers [22]. Nonetheless, the applications of TNTAs were retarded by the wide bandgap (E_g) energy (ca. 3.2 eV) of TiO_2 which can only be excited by UV light irradiation. Hence, it is essential to shift the photoresponse of TiO_2 from UV region to visible scope which may significantly promote the photocatalytic and photoelectrochemical properties of TiO_2-based nanomaterials [23]. To this end, modification of the electronic structure of TNTAs with nonmetal element doping to narrow its bandgap energy has provided a convenient way to solve the disadvantage of TiO_2, most of which centers on carbon [24], nitrogen [25, 26], phosphorus–fluorine [27], and nitrogen–fluorine–iodine doping [28], which result in remarkably enhanced visible-light-driven photocatalytic performances of the materials.

N-doped TNTA nanocomposites have been fabricated for photocatalytic explorations under visible light irradiation [29]. The N-modified TNTAs can be prepared by annealing TNTAs in a urea atmosphere or by anodization in nitrogen-containing electrolytes [30]. The N-implanted TNTAs have been well demonstrated to be the most efficient visible-light-driven photocatalyst among various nonmetal element-doped TNTAs since the nitrogen p states placed just above the valence band maximum of TiO_2 may contribute to the bandgap narrowing without substantial increase of the charge career recombination.

Sulfur doping can also facilitate similar bandgap narrowing; nevertheless, the ionic radius of sulfur was found to be too large to be introduced into TiO_2 lattice as proved by larger formation energy need for the substitution of sulfur than that need for the substitution of N. For example, Tang and Li fabricated S-doped TNTAs by annealing TNTAs in a H_2S atmosphere, and the result showed that sulfur-modified TNTAs demonstrate more pronounced response over the visible light scope leading to significantly enhanced photoelectrochemical signals [31]. Carbon-doped TNTAs were fabricated by oxidation of TNTAs in a burning flame [32] or in CO gas flow [33] or under an argon and acetylene gas mixture flow [34], which endows TNTAs with improved photocatalytic performances under visible light irradiation.

Boron doping was also found to reinforce the visible-light-driven photocatalytic activities, as reported by Lu and co-workers [35] who prepared B-doped TNTAs via chemical vapor deposition approach, in which trimethyl borate was used as boron source and N_2 as carrier gas. It was found that UV–vis spectra of B-doped TNTA nanostructures exhibited a relatively small absorption edge shift toward visible region (385–405 nm) when compared with the large shift observed in N-doping and C-doping TNTAs [36].

5.3.2 TNTAs with Metal Element Doping

Another efficient way to extend the photoresponse of TiO_2 to visible region is doping of TiO_2 with transitional metal ions or rare early metal ions [37, 38]. Extrinsic energy levels in the bandgap of TiO_2 can be formed by incorporation of metal ions into TiO_2 lattice, which may greatly influence the transfer of photogenerated

electrons and holes. Generally, doped metal ions locate near TiO_2 surface to facilitate charge transferring in which the energy level of metal ion reduction should be less negative than the conduction band edge of TiO_2 and the energy level of metal oxidation should be less positive than the valence band edge of TiO_2. Noteworthily, there exists the optimum concentration for metal ion doping, above which the photoactivity decreases owing to recombination of charge carriers in the site of metal ion [39, 40]. With respect to the fabrication of metal ion-doped TNTAs, it is essential to develop applicable approach to efficiently introduce metal ions into TNTAs without changing the vertically oriented morphology of TNTAs. For instance, Zn-doped TNTAs were achieved by immersing TNTAs in Zn-containing solution followed by calcination, as carried out by Yang and co-workers [41]. Zr-doped TNTAs can be fabricated via an electrochemical strategy based on their similar atomic radii (Ti, 2 Å; Zr, 2.16 Å) and belonging to both IV B elements and tetravalentine (+4) elements. W-doped TNTAs were prepared by anodization of tungsten titanium foil, and the red shift of the absorbance edge and a reduction in bandgap (0.14 eV) result in enhanced photocurrent density in comparison with blank TNTAs [42]. Alternatively, Cr-doped TNTAs attained by ion implantation exhibited a significant enhancement in photocurrent response within both UV and visible regions [43].

Few works involving the preparation of Fe-doped TNTAs have been reported, except that Sun and co-workers [44] prepared Fe^{3+}-doped TNTAs by anodization of Ti foil in HF-aqueous electrolyte containing ferric nitrate. Similarly, Li and co-workers [45] prepared Fe-doped TNTAs by anodization of Ti foil in F^- containing aqueous electrolytes of ferrous sulfate. It was found that the Fe-doped TNTAs demonstrate enhanced photocurrent response as compared with blank TNTAs.

5.3.3 TNTA/Noble Metal Nanocomposites

It has been ascertained that modification of TNTAs with noble metal nanoparticles (NPs) renders TNTA/metal nanocomposites efficient photocatalysts leading to significantly enhanced photocatalytic and photoelectrochemical performances [46]. Up to now, TiO_2 has been deposited with various metal NPs such as Pt [47, 48], Au [49, 50], Pd [51], Ag [52, 53], and Co–Ag–Pt [54]. Deposition of metal NPs on the TNTA substrate is beneficial for retarding the recombination of photoexcited electron and hole charge carriers, in which metal NPs can serve as "electron reservoirs" for capturing the photogenerated electrons, thus giving rise to improved photocatalytic performances. For example, with respect to Ag-loaded TNTA nanocomposites, the conduction band (CB) of TiO_2 is lower than the Fermi level of metallic Ag which allows for the transport of photogenerated electrons from CB of TiO_2 to Ag forming a Schottky barrier between TNTAs and Ag NPs [55, 56]. The photogenerated electrons trapped by Ag NPs could be transferred to

the adsorbed oxygen on the Ag surface resulting in O_2^- active species which favor the photocatalytic process. Simultaneously, holes collected in the valence band of TiO_2 could react with water to yield hydroxyl radicals which oxidize pollutants to CO_2 and water, thereby fulfilling the whole photocatalytic cycle.

On the other hand, with regard to the preparation of metal/TNTA nanocomposites, the challenges of synthetically controlling the monodispersivity and homogeneous site distribution of metal NPs on the TNTAs still met with limited success. In particular, uniform deposition of metal NPs on the interior surfaces of TNTAs has been evidenced to be rather difficult than that on the outer surface [57]. Meanwhile, conventional synthetic methods such as complicated photoreduction [58–60] or chemical reduced approach [61] continued to plague the fabrication of well-defined metal/TNTA nanomaterials owing to poor repeatability. Therefore, achieving monodispersed deposition of metal NPs on the TNTAs is highly desirable. To this end, a facile, precisely controlled, and repeatable layer-by-layer (LBL) assembly route was developed to fabricate hierarchically ordered metal/TNTA heterostructures, M/TNTAs (M = Au, Ag, Pt). It was found that the tailor-made metal (Au, Ag, Pt) colloidal NPs were uniformly deposited on the TNTAs through the self-assembly monolayer (SAM) of LBL buildup, as shown in Fig. 5.1, which is afforded by substantial electrostatic attractive interaction between metal NPs and polyelectrolytes. Moreover, photoactivity of these well-defined heterostructures can be tuned by deposition cycles in the LBL process

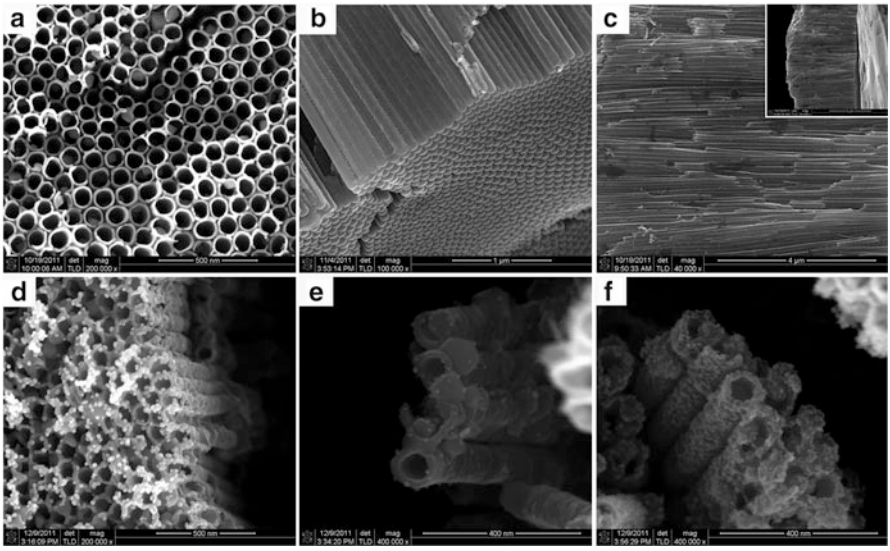

Fig. 5.1 (**a**) Panoramic, (**b**) bottom, and (**c**) magnified cross-sectional SEM images of TNT substrate post-treated by calcination at 450 °C in air for 3 h with corresponding overall cross-sectional view in the inset of (**c**). Top-view SEM images of (**d**) Au/TNT, (**e**) Ag/TNT, and (**f**) Pt/TNT hybrid nanostructures prepared via LBL assembly method (Reprinted with the permission from Ref. [62]. Copyright 2012, American Chemical Society)

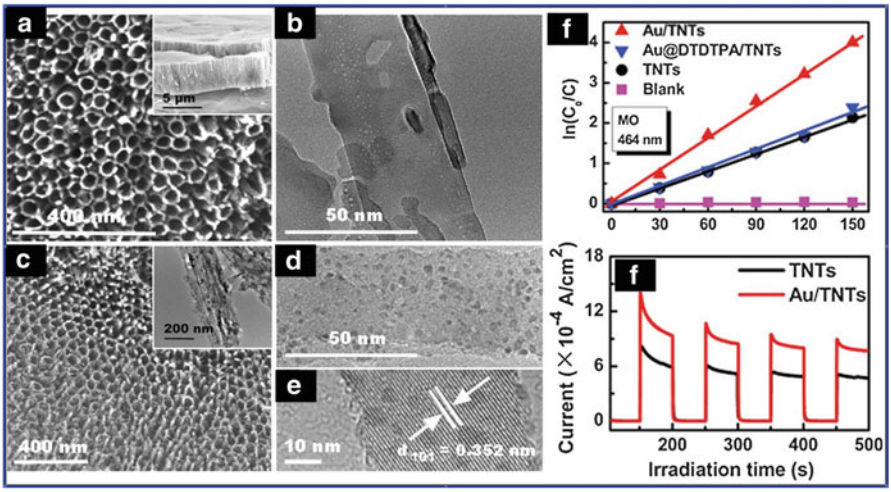

Fig. 5.2 (**a**) Panoramic SEM and (**b**–**c**) TEM views of blank TNTs with cross-sectional image in the inset of (**a**), (**d**) SEM and (**e**) TEM views of the Au/TNT heterostructure. (**f**) Photocatalytic performances of TNT, Au@DTDTPA/TNT, and Au/TNT heterostructure and (**g**) transient photocurrent response of TNT and Au/TNT heterostructure in 0.1 M Na_2SO_4 aqueous solution under UV light irradiation (365 ± 15 nm). The potential of the working electrode was set at 0.0 V versus the Pt counter electrode (Reprinted with permission from Ref. [64]. Copyright 2012, Royal Society of Chemistry)

[62, 63]. Apart from the LBL assembly approach, another facile and green deposition strategy was also developed to achieve the preparation of Au/TNTAs, in which the negatively charged surface ligands of Au NPs were used as linking medium to facilitate the uniform deposition of Au NPs on the positively charged TNTA framework, as shown in Fig. 5.2 [64]. The as-assembled Au/TNTA heterostructure demonstrates significantly enhanced photocatalytic performances under UV light irradiation in comparison with blank TNTAs, for which Au NP deposited intimately on the TNTA substrate is speculated to serve as "electron trap" leading to enhanced separation of photogenerated electron–hole pairs. In another similar work, a facile self-assembly approach based on chemical bonding was developed to synthesize Au/TNTA binary nanostructures, in which Au NPs capped with dodecanethiol (DDT) linker were tethered to the interior and exterior surfaces of TNTAs via 3-mercaptopropionic acid (MPA) molecular which possesses bifunctional groups, as shown in Fig. 5.3. The ensemble of results indicated that the Au/TNTA nanocomposite obtained via the self-assembly approach exhibits significantly enhanced photocatalytic performance as compared to the counterparts of blank TNTAs, P25 particulate film, flat anodic TiO_2 layer (FTL), and Au/FTL owing to the well-dispersed deposition of Au on the TNTA matrix, in which Au components play crucial roles as "electron reservoirs" and, simultaneously, the conducting Ti substrate beneath the nanotubes is conducive to electron transport, thus concurrently reinforcing the separation of photogenerated electron–hole pairs.

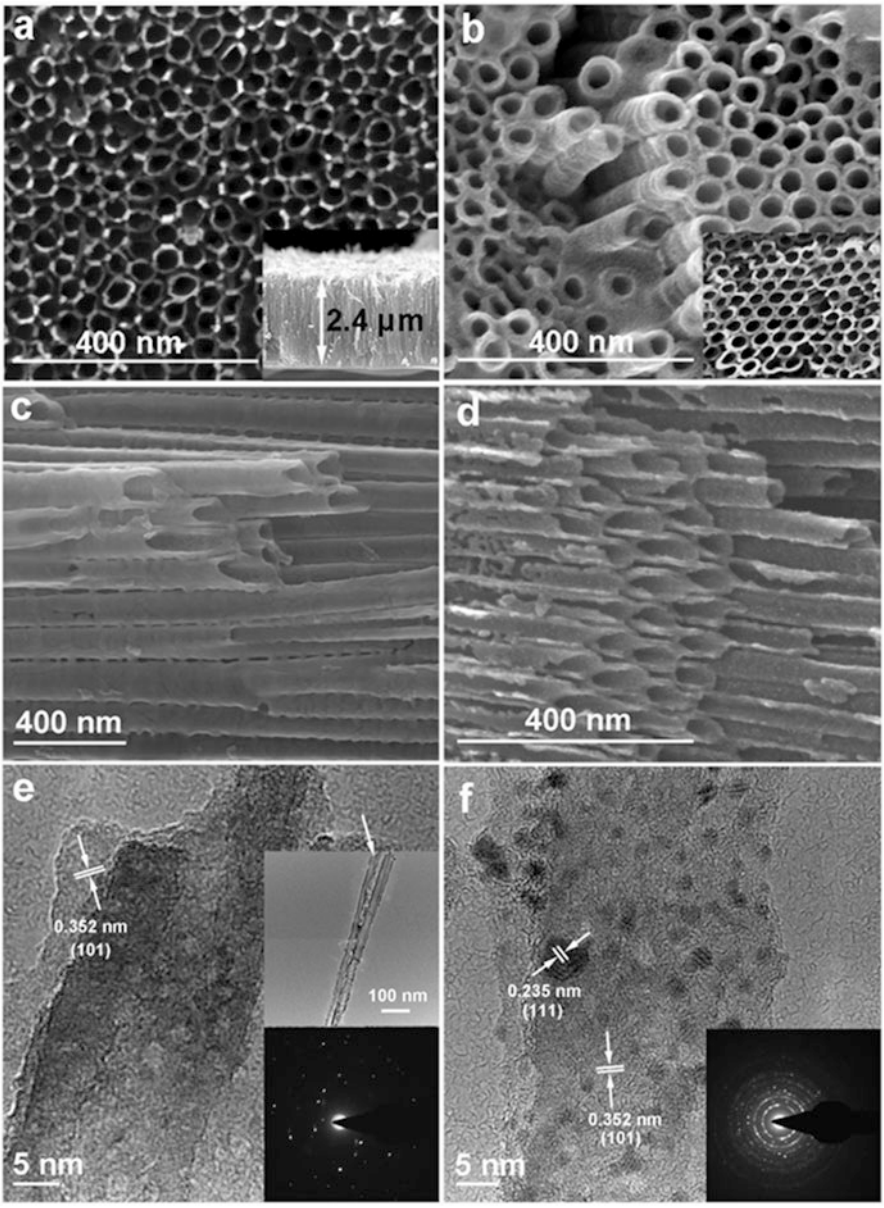

Fig. 5.3 Typical panoramic SEM views of (**a**) vertically oriented TNTAs post-treated with calcination at 450 °C in air for 3 h with cross-sectional image in the inset and (**b**) Au/TNTAs (1.14 wt%) with additional detailed image in the inset; magnified cross-sectional SEM images of (**c**) TNTAs and (**d**) Au/TNTAs; HRTEM images of (**e**) TNTAs and (**f**) Au/TNTAs with corresponding SAED patterns in the inset (Reprinted with permission from Ref. [91]. Copyright 2012, Royal Society of Chemistry)

This work affords a facile and efficient strategy to prepare a large variety of metal/TNTA nanocomposites via similar surface modification.

5.3.4 TNTA/Plasmonic Metal or Metal Cluster Nanocomposites

In recent years, plasmonic energy conversion was proposed as a promising route to conventional electron–hole separation in semiconductors [65]. The key to utilize the plasmonic effect of metal component in photocatalysis is the controlled spatial distribution of monodispersed metal NPs on the semiconductor matrix. Till now, there have been some promising results on the applications of plasmonic effect to enhance the photoactivities of TNTAs, such as visible-light-driven Ag/AgCl/TNTA nanocomposite [66]. In such a ternary heterostructure, a new surface-plasmon-induced photocatalytic mechanism was presented for the remarkably enhanced photocatalytic performance of Ag/AgCl/TNTA nanocomposite, in which Ag NPs with a mean diameter of 20 nm were speculated to be photoexcited owing to plasmonic resonance, followed by the transfer of photogenerated electrons from Ag NPs to the conduction band of TiO_2 and, simultaneously, the transfer of compensative electrons from electron donor (Cl^-) to the Ag NPs, thereby resulting in pronouncedly enhanced photoactivities of the ternary nanostructure [67].

Besides, a new class of nanomaterial-metal cluster, consisting of precise number of metal atoms protected by thiolate ligands, has recently emerged as a novel photosensitizer to extend the photoactivity of TiO_2. In striking contrast to conventional bulk metallic NPs, metal clusters exhibit (e.g., Au_x clusters) several distinct properties, such as unique atom-packing mode, strong electron energy quantization induced by the ultra-small cluster size, sizable bandgap, and controllable catalytic properties. More recently, glutathione-capped Au_x clusters and highly ordered nanoporous layer-covered TNTAs (NP-TNTAs) were employed as nanobuilding blocks for the construction of well-defined Au_x/NP-TNTA heterostructures via a facile electrostatic self-assembly strategy. Versatile photocatalytic performances of the Au_x/NP-TNTA heterostructure which acts as a model catalyst, including photocatalytic oxidation of organic pollutants, photocatalytic reduction of aromatic nitro compounds, and photoelectrochemical (PEC) water splitting under simulated solar light irradiation, were systematically exploited [68]. It was found that synergistic interaction stemming from monodisperse coverage of Au_x clusters on NP-TNTAs in combination with hierarchical nanostructure of NP-TNTAs reinforces light absorption of Au_x/NP-TNTA heterostructure especially within visible region, hence contributing to the significantly enhanced photocatalytic and PEC water splitting performances.

5.3.5 TNTA/Semiconductor Nanocomposites

A formidable challenge still remains in reducing the quick recombination rate of photogenerated electron–hole pairs over TiO_2. Although transformation of TiO_2 morphology to nanotubular structure may open a convenient avenue to improve the photocatalytic efficiency, it cannot tackle the central issue of photocatalysis [69]. Therefore, various research activities have devoted to reinforcing the photocatalytic properties by synthesizing TNTA/semiconductor hybrid nanostructures [70, 71]. For example, nanosized judicious coupling of TiO_2 and ZnO has been well established to remarkably enhance the separation efficiency of photoexcited charge carriers due to the formation of heterojunction structure between them [72, 73], thereby boosting quantum efficiency and photostability of the hybrid photocatalyst [74, 75].

Inspired by this, combined with structural advantages of vertically aligned TNTA framework (e.g., high specific surface area and excellent chemical stability) as starting nanobuilding blocks, hierarchical ordered ZnO/TNTA composite photocatalysts with promising photocatalytic performances could be attained. Numerous chemical, electrochemical, and physical approaches have been developed to fabricate the ZnO/TNTA hybrid nanomaterials, including template-assisted strategy [76–78], hydrothermal method [79, 80], electrodeposition approach [81], and filtered cathodic-vacuum-arc technique [82]. Besides, Xiao et al have developed an efficient one-step pyrolysis route to fabricate 1D hierarchical ZnO/TNTA heterostructures, by which in situ formed ZnO nanocrystals were uniformly grafted on the framework of TNTAs [83]. The results show that enhanced separation of electron–hole pairs and improved photostability of the ZnO/TNTA heterostructures were achieved. The morphologies of the hierarchical nanostructures of ZnO/TNTA heterostructure were illustrated in Fig. 5.4.

In another work, spatially hierarchically ordered ZnO nanorod (NR)-decorated NP-TNTA (ZnO NR/NP-TNTA) nanocomposites have been prepared by an efficient, two-step anodization route combined with an electrochemical deposition strategy, by which monodispersed one-dimensional (1D) ZnO NRs were uniformly grown on the framework of NP-TNTA substrate, as shown in Fig. 5.5 [84]. It was found that the ZnO NR/NP-TNTA heterostructure exhibits significantly enhanced photocatalytic and photoelectrocatalytic performances, along with favorable photostability toward degradation of organic pollutants under UV light irradiation, as compared to the single-component counterparts. The remarkably enhanced photoactivity of ZnO NR/NP-TNTA heterostructure is ascribed to the intimate interfacial integration between ZnO NR and NP-TNTA substrate imparted by the unique spatially branched hierarchical structure, thereby contributing to the efficient transfer and separation of photogenerated electron–hole charge carriers.

Moreover, many other narrow-bandgap semiconductors have also been used to sensitize the NP-TNTAs, for example, a hierarchically ordered CdSe/NP-TNTA hybrid nanostructure was fabricated through a facile electrochemical deposition strategy, by which the CdSe ingredients, consisting of clusters of quantum dots (QDs), were uniformly assembled on the inner and outer surfaces of the NP-TNTA framework, as revealed by Fig. 5.6 [85]. It was demonstrated that the as-prepared

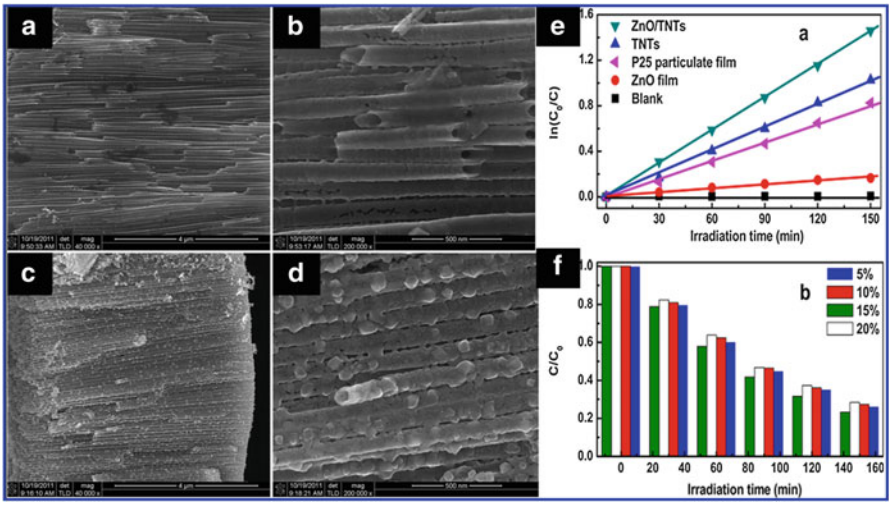

Fig. 5.4 Panoramic views of (**a**) TNTs fabricated via two-step anodization approach and the as-prepared (**b**) ZnO/TNT heterostructure; cross-sectional images of (**c** and **e**) TNT and (**d** and **f**) ZnO/TNT heterostructure (15 %); (**e**) photocatalytic activities of TNT, ZnO film, and ZnO/TNT heterostructure (15 %), and P25 particulate film for photodegradation of RhB aqueous solution under ambient conditions. (**f**) Photocatalytic performance of the ZnO/TNT heterostructure with varied deposition percentage of $Zn(NO_3)_2$ precursor in ethanol aqueous solution (Reprinted with the permission from Ref. [83]. Copyright 2012, American Chemical Society)

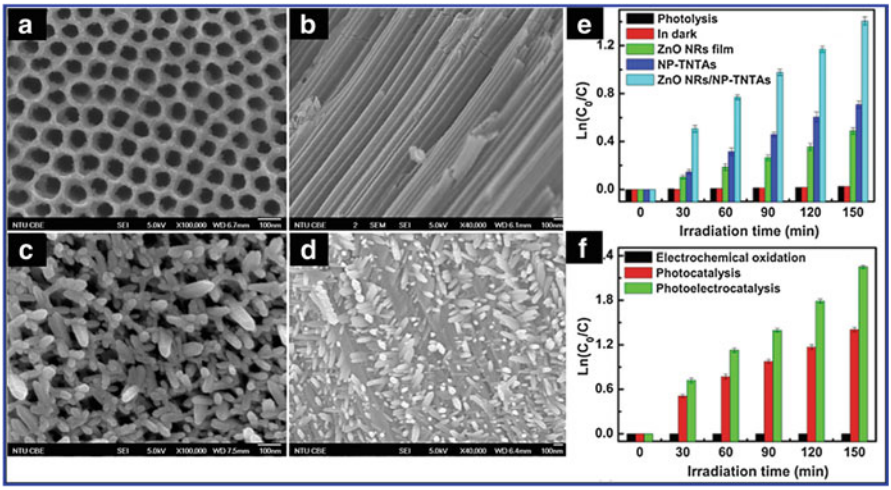

Fig. 5.5 Panoramic FESEM images of (**a**) NP-TNTA and (**c**) spatially branched hierarchical ZnO NR/NP-TNTA heterostructure, and cross-sectional images of (**b**) NP-TNTA and (**d**) ZnO NR/NP-TNTA heterostructure. (**e**) Photocatalytic performances of blank NP-TNTAs, pure ZnO NR film, and spatially branched hierarchical ZnO NR/NP-TNTA heterostructure toward degradation of RhB under UV light irradiation (365 ± 15 nm), (**f**) photocatalytic and photoelectrocatalytic activities of ZnO NR/NP-TNTA heterostructure under UV light irradiation (365 ± 15 nm) (Reprinted with permission from Ref. [84]. Copyright 2014, Royal Society of Chemistry)

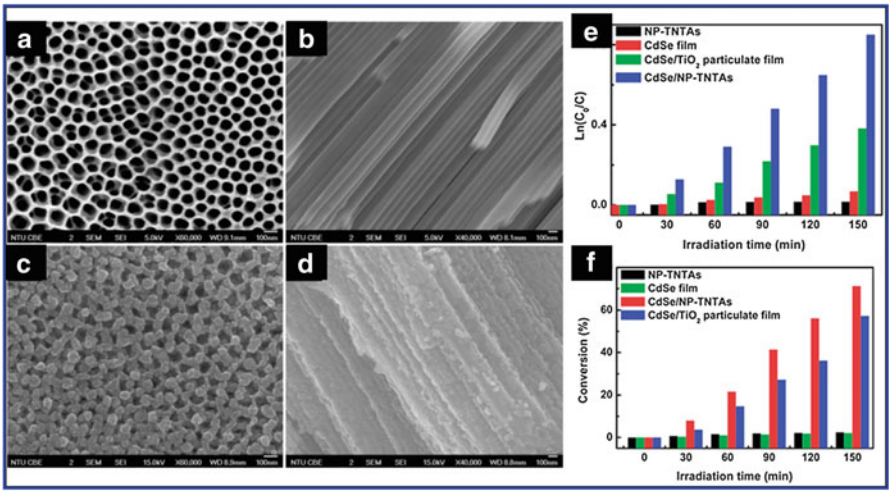

Fig. 5.6 FESEM images of (**a** and **b**) NP-TNTA and (**c** and **d**) CdSe/NP-TNTA heterostructure prepared via electrochemical deposition with deposition time of 1600s. (**e**) Photocatalytic performances of different samples and (**f**) photocatalytic reduction of 4-NA over different samples under visible light irradiation ($\lambda > 420$ nm) with the addition of ammonium formate as quencher for photogenerated holes and N_2 purge under ambient conditions (Reprinted with permission from Ref. [85]. Copyright 2014, Royal Society of Chemistry)

CdSe/NP-TNTA heterostructure could serve as an efficient photoanode for photoelectrochemical water splitting, and, moreover, it could also be used as a multifunctional photocatalyst for photoredox applications, including photocatalytic oxidation of organic dye pollutants and selective reduction of aromatic nitro compounds under visible light irradiation. Similarly, tailor-made negatively charged CdS QDs were evenly deposited on a hierarchical framework of NP-TNTAs by modulating surface charge properties of constituents, as displayed in Fig. 5.7. It has been demonstrated that the CdS/NP-TNTA hybrid nanostructures exhibit promising visible-light-driven photoactivity toward photooxidation of organic dye pollutants and photocatalytic reduction of nitrophenol derivatives as a result of monodisperse deposition of CdS QDs on the well-defined NP-TNTA scaffold [86].

5.4 Photocatalytic Applications of TNTA-Based Nanocomposites

5.4.1 Nonselective Degradation of Organic Dye Pollutants

Nonselective photocatalysis has been extensively investigated owing to its great significance to environmental remediation [5, 87–89], by which contaminants are mineralized to less toxic inorganic compounds, such as water, carbon dioxide, and

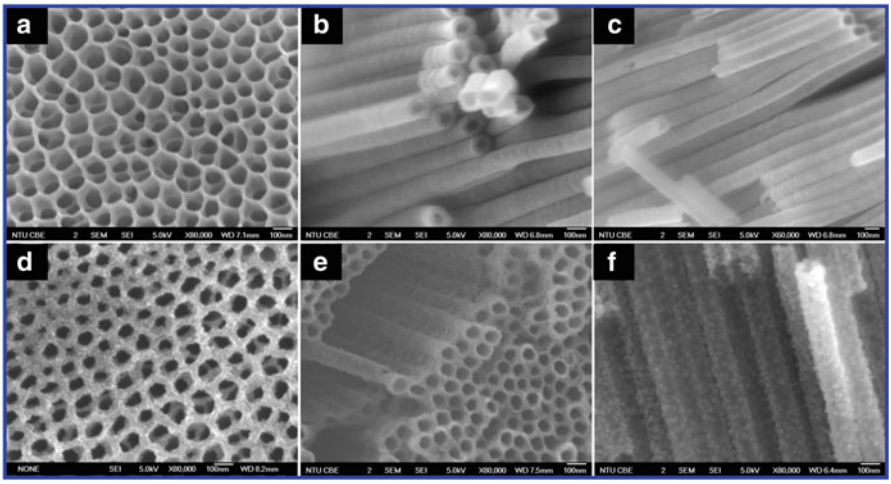

Fig. 5.7 Panoramic FESEM images of (**a**) NP-TNTAs and (**d**) CdS QD/NP-TNTAs and cross-sectional FESEM images of (**b** and **c**) NP-TNTAs, (**e** and **f**) CdS QD/NP-TNTA heterostructure (Reprinted with permission from Ref. [86]. Copyright 2013, Royal Society of Chemistry)

salts [90]. A series of 1D noble metal/TiO_2 nanocomposites (with mean diameter of 14.7, 6.3, and 3.1 nm for Au, Ag, and Pt, respectively.) have been prepared via a facile and easily accessible electrostatic self-assembly approach by tuning surface charge properties of the hierarchically ordered TNTAs, as shown in Fig. 5.8 [62–64, 91]. These 1D hybrid nanostructures exhibited substantially enhanced photocatalytic performances toward degradation of organic dye pollutants owing to the Schottky barrier effect of noble metal NPs, which provides a new strategy to design highly ordered metal/1D semiconductor binary nanocomposites based on electrostatic interaction.

5.4.2 Selective Organic Transformation

Selective organic transformation is of great industrial importance owing to the extensive use of organics in diverse applications. In particular, photocatalytic selective organic transformation is a green and promising technique, exhibiting intrinsic merits including mild reaction conditions and the possibility to reduce the generation of undesired by-products. More recently, TNTAs modified with ultra-small Au_x clusters has been utilized as an efficient photocatalyst for selective reduction of a series of aromatic nitro compounds to corresponding amino compounds under simulated solar light irradiation [68]. It was speculated that the photogenerated electrons photoexcited from the HOMO (highest occupied molecular orbital) to LUMO (lowest unoccupied molecular orbital) of Au_x clusters under simulated solar light irradiation transfer to the conduction band of TiO_2 which

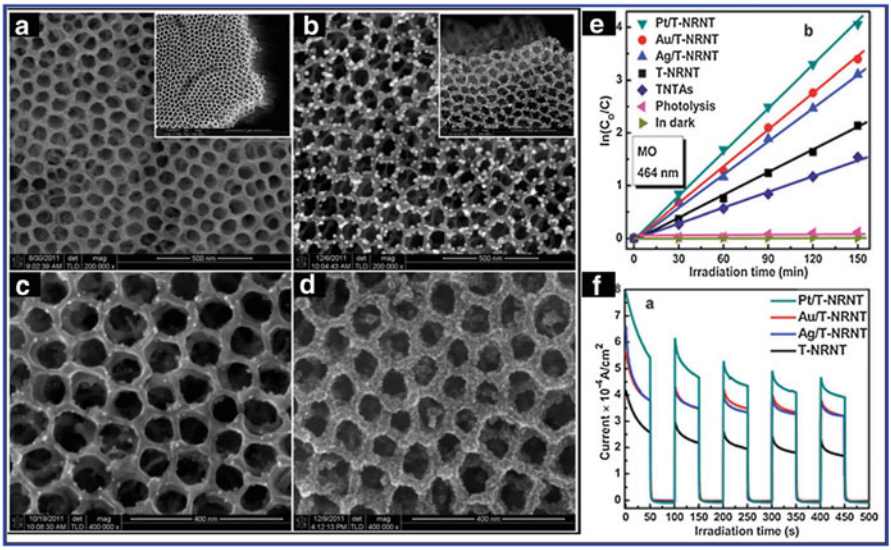

Fig. 5.8 (**a**) Panoramic view of T-NRNT attained via the 2nd anodization with cross-sectional view in the inset, (**b**) high-resolution images of Au/T-NRNT with cross-sectional view in the inset, (**c**) Ag/T-NRNT, and (**d**) Pt/T-NRNT fabricated via a LBL self-assembly approach. (**e**) Photocatalytic performances of M/T-NRNT (M = Au, Ag, Pt) and (**f**) transient photocurrent responses of T-NRNT and M/T-NRNT (M = Au, Ag, Pt) heterostructures in 0.1 M Na_2SO_4 aqueous solution under UV light irradiation (365 ± 15 nm) (Reprinted with permission from Ref. [63]. Copyright 2012, Royal Society of Chemistry)

reduces the nitro compounds absorbed on the scaffold of TNTAs to amino compounds, as clearly displayed in Fig. 5.9. Noteworthily, the selective photocatalytic reactions were performed in a N_2 atmosphere, and photogenerated holes were completely quenched by hole scavengers; thus all photoinduced electrons in the reaction system were involved in the selective photoreduction reactions. Similar organic transformation reactions were also observed on the CdS QDs/NP-TNTAs which demonstrated significantly enhanced photoreduction performances under visible light irradiation in comparison with blank NP-TNTAs [86].

5.4.3 CO_2 Reduction

Solar-energy-driven conversion of CO_2 into hydrocarbon fuels can simultaneously generate chemical fuels to meet energy demand and mitigate rising CO_2 levels. Thus far, diverse ranges of 1D nanostructures have been used for photoreduction of CO_2 into chemical fuels [92–94], among which TNTAs were found to efficiently convert CO_2 and water vapor into methane and other hydrocarbons under outdoor sunlight irradiation [92]. Specifically, Shankar's group demonstrated an approach that is able to achieve high-rate sunlight-driven conversion of diluted CO_2 to light

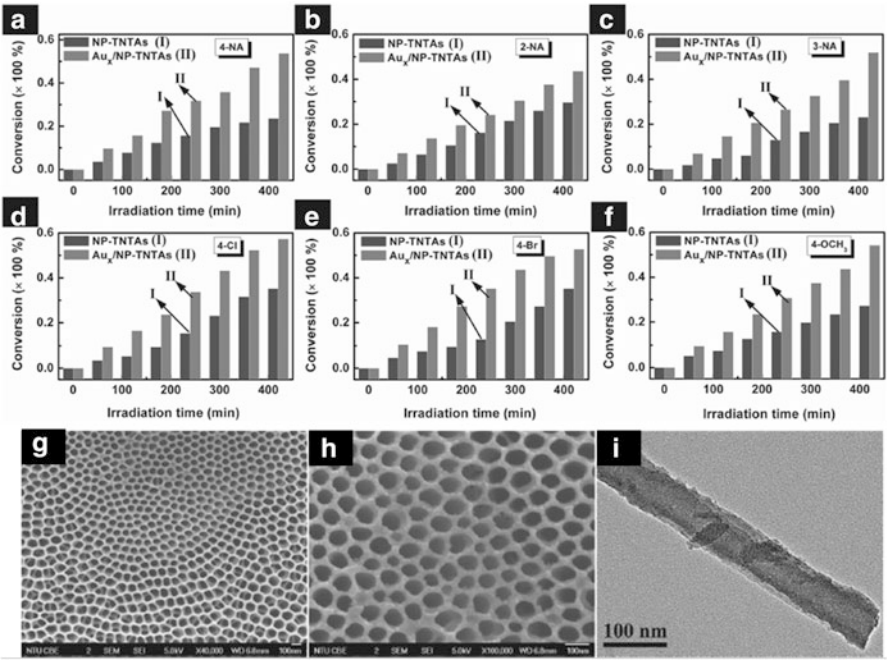

Fig. 5.9 Photocatalytic reduction of substituted aromatic nitro compounds over blank NP-TNTA and Au_x/NP-TNTA heterostructure (with dipping time for 96 h) under simulated solar light irradiation, with the addition of ammonium formate as quencher for photogenerated holes and N_2 purge under ambient conditions: (**a**) 4-nitroaniline (4-NA), (**b**) 3-nitroaniline (3-NA), (**c**) 2-nitroaniline (2-NA), (**d**) 1-chloro-4-nitrobenzene (4-Cl), (**e**) 1-bromo-4-nitrobenzene (4-Br), and (**f**) 4-nitroanisole (4-OCH_3). (**g** and **h**) Panoramic FESEM images of Au_x/NP-TNTA heterostructure. (**i**) Low-magnified TEM image of Au_x/NP-TNTA heterostructure (Reproduced from Ref. [68] by permission of John Wiley & Sons, Ltd)

hydrocarbons in which an optimized combination of a Cu–Pt coating and modulated-diameter TiO_2 nanotube was used as photocatalyst. Their results showed that at least fourfold improvement in CO_2 conversion rates over prior art using a catalyst consisting of coaxial Cu–Pt bimetallic shells supported on a periodically modulated double-walled TNTA (PMTiNT) core. Under AM 1.5 one-sun illumination, a hydrocarbon production rate of 3.51 mL g^{-1} h^{-1} or 574 nmol cm^{-2} h^{-1} using 99.9 % CO_2 was attained, as shown in Fig. 5.10. Moreover, the periodic modulation of the diameters of the TNTAs increased the surface area and improved the utilization of light, while the bimetallic coating increased catalyst activity and specificity [92]. In another work, nitrogen-doped TNTAs were used for photocatalytic conversion of CO_2 and water vapor to hydrogen fuels. Using outdoor global AM 1.5 sunlight (100 mW/cm^2), a hydrocarbon production rate of 111 ppm cm^{-2} h^{-1}, or $\approx$ 160 μL/(g h), was obtained when the nanotube arrays were loaded with both Cu and Pt nanoparticles [95, 96]. This work suggested that high-rate photocatalytic conversion of CO_2 can be achieved using sunlight and

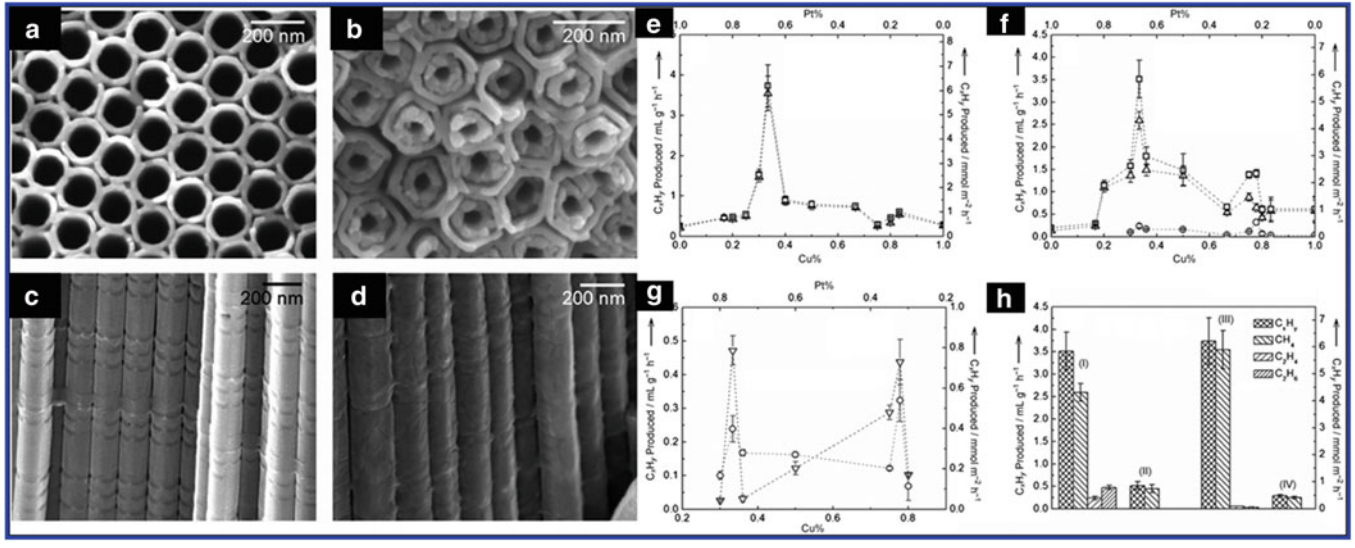

Fig. 5.10 (**a** and **b**) Plan-view and (**c** and **d**) cross-sectional SEM images of the as-prepared PMTiNT platform (**a** and **c**) and Cu–Pt loaded nanotubes (**b** and **d**). (**e** and **f**) Plots of hydrocarbon (□), CH_4 (△), and C_2H_4 (○) solar-driven generation rates against fraction of Cu in Cu–Pt bimetallic system using 0.998 % (**e**) and 99.9 % (**f**) CO_2. (**g**) Comparison of the C_2H_4 (○) and C_2H_6 (▽) solar-driven generation rates against fraction of Cu in the Cu–Pt bimetallic system using 99.9 % CO_2. (**h**) Comparison of hydrocarbon generation activities of $Cu_{0.33}$–$Pt_{0.67}$ nanotube-loaded PMTiNTs (I, III) and regular TiNTs (II, IV) using 99.9 % (I, II) and 0.998% (III, IV) CO_2 (Reproduced from Ref. [92] by permission of John Wiley & Sons, Ltd)

high-surface-area TNTAs, with a nanotube wall thickness less than or in the range of the minority carrier-diffusion length, in combination with co-catalyst nanoparticles coated on the nanotube array surface. These two works open new avenues for carbon recycling using renewable sources.

5.4.4 Photoelectrochemical (PEC) Water Splitting

The aligned porosity, crystallinity, and oriented nature of the nanotubular structure make TNTAs an ideal candidate for promising PEC applications. The intrinsic configuration of TNTAs affords significantly shorter carrier-diffusion paths along the nanotube wall and minimizes the occurrence of charge losses arising from the electron hopping between nanoparticles [97, 98]. Moreover, the freestanding TNTAs are grown vertically on Ti substrate which can be directly used as photoelectrodes. In the past few years, construction of TNTA-based photoelectrode for PEC water splitting has been gaining continuous interest. For example, a visible-light-responsive plasmonic photocatalytic composite photoelectrode was constructed by rationally selecting Au nanocrystals (20 nm) and assembling them onto TNTA-based photonic crystal substrate with a pore diameter of 200 nm (Fig. 5.11) [99]. The rational design of the composite materials remarkably increased the SPR intensity of Au and consequently promoted the hot-electron

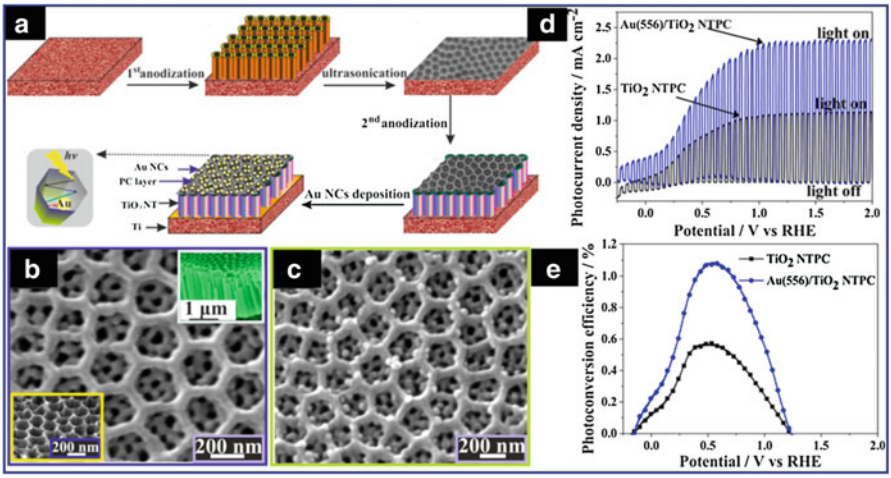

Fig. 5.11 (**a**) Schematic diagram showing the fabrication procedure for Au/TiO_2 nanotube photonic crystals (NTPC). (**b**) SEM images of TiO_2 NTPC, top right inset shows a cross-sectional view and bottom left inset shows high magnification of tilt 15° cross-sectional view of top PC layer, and (**c**) SEM image of Au/TiO_2 NTPC. (**d**) Linear-sweep voltammograms of the samples under chopped AM 1.5G irradiation with a scan rate of 5 mV/s, and (**e**) photoconversion efficiency as a function of applied potential (Reprinted with the permission from Ref. [99]. Copyright 2013, American Chemical Society)

injection from Au nanocrystals into CB of TiO_2, thus resulting in substantially enhanced PEC water splitting performances under visible light irradiation ($\lambda > 420$ nm). In another work, TNTAs modified with palladium quantum dots (Pd QDs, 3.3 ± 0.7 nm) demonstrated substantially increased monochromatic incident photon-to-electron conversion efficiency (IPCE) of nearly 100 % at $\lambda = 330$ nm [100]. It was speculated that the synergistic interaction between nanotubular structure of TNTAs and uniformly dispersed Pd QDs facilitated the charge transfer of photogenerated electrons from TNTAs to Pd QDs and, simultaneously, the high activity of Pd QDs acting as catalytic centers contributed to the high-efficiency PEC hydrogen production. Apart from TNTAs, multicomponent nanotube arrays such as vertically oriented Ti–Pd mixed oxynitride nanotube arrays [101], Ti–Fe–O nanotube arrays [102], Ti–Nb–Zr–O mixed oxide nanotube arrays [103], and Ta_3N_5 nanotube arrays [104] have also been studied for PEC water splitting under simulated solar light or visible light irradiation.

5.5 Conclusions

In summary, TNTA-based nanostructures have emerged as promising photocatalysts for utilizing solar energy in the field of photocatalysis owing to their structural advantages including high surface-to-volume ratios and unique nanotube array structures. This chapter briefly introduces the state-of-the-art developments of TNTAs which mainly concentrate on the modification strategies and photocatalytic applications of TNTA-based nanocomposites. These judiciously modified TNTA nanostructures exhibit improved UV and visible light absorption, thus harvesting an increased portion of solar spectrum and reducing the recombination of photogenerated electron–hole pairs. Future research efforts may be directed to fabricate TNTAs of different chemical compositions with good chemical and physical stabilities to absorb a broader solar spectrum, especially the infrared region which accounts for a large portion of the solar spectrum. It is anticipated that TNTA-based hybrid nanostructures could afford more versatile potential applications in a myriad of fields.

References

1. Liu C, Dasgupta NP, Yang P (2014) Semiconductor nanowires for artificial photosynthesis. Chem Mater 26:415–422
2. Wang M, Ioccozia J, Sun L et al (2014) Inorganic-modified semiconductor TiO_2 nanotube arrays for photocatalysis. Energy Environ Sci 7:2182–2202
3. Fujishima A, Honda K (1972) Electrochemical photolysis of water at a semiconductor electrode. Nature 238:37–38
4. Zhang Y, Zhang N, Tang Z-R et al (2012) Visible-light-driven oxidation of primary C–H bonds over CdS with dual co-catalysts graphene and TiO_2. Chem Sci 3:2812–2822

5. Zhang Y, Tang Z-R, Fu X et al (2010) TiO_2-graphene nanocomposites for gas-phase photocatalytic degradation of volatile aromatic pollutant: is TiO_2-graphene truly different from other TiO_2-carbon composite materials? ACS Nano 4:7303–7314
6. Hochbaum AI, Chen R, Delgado RD et al (2008) Enhanced thermoelectric performance of rough silicon nanowires. Nature 451:163–167
7. Zhang Z, Yu Y, Hedhili MN (2012) Microwave-assisted self-doping of TiO_2 photonic crystal for efficient photoelectrochemical water splitting. ACS Appl Mater Interfaces 4:990–996
8. Zhu K, Vinzant TB, Neale NR et al (2007) Removing structural disorder from oriented TiO_2 nanotube arrays: reducing the dimensionality of transport and recombination in dye-sensitized solar cells. Nano Lett 7:3739–3746
9. Albu SP, Ghicov A, Macak JM et al (2007) Self-organized, free-standing TiO_2 nanotube membrane for flow-through photocatalytic applications. Nano Lett 7:1286–1289
10. Asahi R, Morikawa T, Ohwaki T et al (2001) Visible-light photocatalysis in nitrogen-doped titanium oxides. Science 293:269–271
11. Qin WP, Zhang DS, Zhao D et al (2010) Near-infrared photocatalysis based on YF_3:Yb^{3+}, Tm^{3+}/TiO_2 core/shell nanoparticles. Chem Commun 46:2304–2306
12. Wu Y, Liu H, Zhang J et al (2009) Enhanced photocatalytic activity of nitrogen-doped titania by deposited with gold. J Phys Chem C 113:14689–14695
13. Wang CL, Sun L, Yun H et al (2009) Sonoelectrochemical synthesis of highly photoelectrochemically active TiO_2 nanotubes by incorporating CdS nanoparticles. Nanotechnology 20:295601–295606
14. Wang M, Sun L, Lin Z et al (2013) p–n Heterojunction photoelectrodes composed of Cu_2O-loaded TiO_2 nanotube arrays with enhanced photoelectrochemical and photoelectrocatalytic activities. Energy Environ Sci 6:1211–1220
15. Gong D, Grimes CA, Varghese OK et al (2001) Titanium oxide nanotube arrays prepared by anodic oxidation. J Mater Res 16:3331–3334
16. Cai Q, Paulose M, Varghese OK et al (2005) The effect of electrolyte composition on the fabrication of self-organized titanium oxide nanotube arrays by anodic oxidation. J Mater Res 20:230–235
17. Mor GK, Shankar K, Paulose M et al (2005) Enhanced photocleavage of water using titania nanotube arrays. Nano Lett 5:191–195
18. Parkhutik VP, Shershulsky VI (1992) Theoretical modelling of porous oxide growth on aluminium. J Phys D Appl Phys 25:1258–1263
19. Macdonald DD (1993) On the formation of voids in anodic oxide films on aluminum. J Electrochem Soc 140:27–30
20. Thompson GE (1997) Porous anodic alumina: fabrication, characterization and applications. Thin Solid Films 297:192–201
21. Siejka J, Ortega C (1977) An O^{18} study of field-assisted pore formation in compact anodic oxide films on aluminum. J Electrochem Soc 124:883–891
22. Roy P, Berger S, Schmuki P (2011) TiO_2 nanotubes: synthesis and applications. Angew Chem 50:2904–2940
23. Mohamed AE, Kasemphaibulsuk N, Rohani S et al (2010) Fabrication of titania nanotube arrays in viscous electrolytes. J Nanosci Nanotechnol 10:1998–2008
24. Xu C, Shaban YA, Ingler WB et al (2007) Nanotube enhanced photoresponse of carbon modified (CM)-n-TiO_2 for efficient water splitting. Sol Energy Mater Sol Cells 91:938–943
25. Vitiello RP, Macak JM, Ghicov A et al (2006) N-doping of anodic TiO_2 nanotubes using heat treatment in ammonia. Electrochem Commun 8:544–548
26. Geng J, Yang D, Zhu J et al (2009) Nitrogen-doped TiO_2 nanotubes with enhanced photocatalytic activity synthesized by a facile wet chemistry method. Mater Res Bull 2009 (44):146–150
27. Chen X, Zhang X, Su Y et al (2008) Preparation of visible-light responsive P F-codoped TiO_2 nanotubes. Appl Surf Sci 254:6693–6696

28. Lei L, Su Y, Zhou M (2007) Fabrication of multi-non-metal-doped TiO_2 nanotubes by anodization in mixed acid electrolyte. Mater Res Bull 42:2230–2236
29. Beranek R, Macak JM, Gartner M et al (2009) Enhanced visible light photocurrent generation at surface-modified TiO_2 nanotubes. Electrochim Acta 54:2640–2646
30. Su Y, Zhang X, Zhou M et al (2008) Preparation of high efficient photoelectrode of N–F-codoped TiO_2 nanotubes. J Photochem Photobiol A Chem 194:152–160
31. Tang X, Li D (2008) Sulfur-doped highly ordered TiO_2 nanotubular arrays with visible light response. J Phys Chem C 112:5405–5409
32. Shankar K, Paulose M, Mor GK et al (2005) A study on the spectral photoresponse and photoelectrochemical properties of flame-annealed titania nanotube-arrays. J Phys D Appl Phys 38:3543–3549
33. Park JH, Kim S, Bard AJ (2006) Novel carbon-doped TiO_2 nanotube arrays with high aspect ratios for efficient solar water splitting. Nano Lett 6:24–28
34. Lee HH, Shin SL et al (2008) Effect of gas pressure on Al coatings by cold gas dynamic spray. Mater Lett 62:1579–1581
35. Lu N, Quan X, Li JY et al (2007) Fabrication of boron-doped TiO_2 nanotube array electrode and investigation of its photoelectrochemical capability. J Phys Chem C 111:11836–11842
36. Su Y, Chen S, Quan X et al (2008) A silicon-doped TiO_2 nanotube arrays electrode with enhanced photoelectrocatalytic activity. Appl Surf Sci 255:2167–2172
37. Choi W, Termin A, Hoffmann MR (1994) The role of metal ion dopants in quantum-sized TiO_2: correlation between photoreactivity and charge carrier recombination dynamics. J Phys Chem C 98:13669–13679
38. Dvoranova D, Brezova V, Mazur AM (2002) Investigations of metal-doped titanium dioxide photocatalysts. Appl Catal, B 37:91–105
39. Tu YF, Huang SY, Sang JP (2010) Preparation of Fe-doped TiO_2 nanotube arrays and their photocatalytic activities under visible light. Mater Res Bull 45:224–229
40. Tu YF, Huang SY, Sang JP (2009) Synthesis and photocatalytic properties of Sn-doped TiO_2 nanotube arrays. J Alloys Compd 482:382–387
41. Yang Y, Wang X, Li L (2010) Zinc-doped TiO_2 nanotube arrays. Key Eng Mater 434:446–447
42. Zhao J, Wang X, Kang Y et al (2008) Photoelectrochemical activities of W-doped titania nanotube arrays fabricated by anodization. IEEE Photon Technol Lett 20:1213–1215
43. Ghicov A, Schmidt B, Kunze J et al (2007) Photoresponse in the visible range from Cr doped TiO_2 nanotubes. Chem Phys Lett 433:323–326
44. Sun L, Li J, Wang CL et al (2009) An electrochemical strategy of doping Fe^{3+} into TiO_2 nanotube array films for enhancement in photocatalytic activity. Sol Energy Mater Sol Cells 93:1875–1880
45. Li J, Yun H, Lin CJ (2008) Investigations on the Fe-doped TiO_2 nanotube arrays as a photoanode for cathodic protection of stainless steel. ECS Trans 3:1–9
46. Zhu BL, Guo Q, Huang XL et al (2006) Characterization and catalytic performance of TiO_2 nanotubes-supported gold and copper particles. J Mol Catal A Chem 249:211–217
47. Mussy JPG, Macpherson JV, Delplancke JL (2003) Characterisation and behaviour of Ti/TiO_2/noble metal anodes. Electrochim Acta 2003(48):1131–1141
48. Ikuma Y, Bessho H (2007) Effect of Pt concentration on the production of hydrogen by a TiO_2 photocatalyst. Int J Hydrog Energy 32:2689–2692
49. Furube A, Du L, Hara K et al (2008) Ultrafast plasmon-induced electron transfer from gold nanodots into TiO_2 nanoparticles. J Am Chem Soc 129:14852–14853
50. Milsom EV, Novak J, Oyama M et al (2007) Electrocatalytic oxidation of nitric oxide at TiO_2–Au nanocomposite film electrodes. Electrochem Commun 9:436–442
51. Lee JH, Choi HS, Lee JH et al (2009) Fabrication of titania nanotubular film with metal nanoparticles. J Cryst Growth 311:638–641
52. Sun L, Li J, Wang C et al (2009) Ultrasound aided photochemical synthesis of Ag loaded TiO_2 nanotube arrays to enhance photocatalytic activity. J Hazard Mater 171:1045–1050

53. He BL, Dong B, Li HL (2007) Preparation and electrochemical properties of Ag-modified TiO_2 nanotube anode material for lithium-ion battery. Electrochem Commun 9:425–430
54. Yang L, He D, Cai Q et al (2007) Fabrication and catalytic properties of Co-Ag-Pt nanoparticle-decorated titania nanotube arrays. J Phys Chem C 111:8214–8217
55. Yu J, Xiong J, Cheng B et al (2005) Fabrication and characterization of Ag–TiO_2 multiphase nanocomposite thin films with enhanced photocatalytic activity. Appl Catal B Environ 60:211–221
56. Subramanian V, Wolf E, Kamat PV (2001) Semiconductor-metal composite nanostructures. To what extent do metal nanoparticles improve the photocatalytic activity of TiO_2 films? J Phys Chem B 105:11439–11446
57. Seabold JA, Shankar K, Wilke RHT et al (2008) Photoelectrochemical properties of heterojunction CdTe/TiO_2 electrodes constructed using highly ordered TiO_2 nanotube arrays. Chem Mater 20:5266–5273
58. Paramasivam I, Macak JM, Ghicov A (2007) Enhanced photochromism of Ag loaded self-organized TiO_2 nanotube layers. Chem Phys Lett 445:233–237
59. Paramasivam I, Macak JM, Schmuki P et al (2008) Photocatalytic activity of TiO_2 nanotube layers loaded with Ag and Au nanoparticles. Electrochem Commun 0:71–75
60. Song YY, Gao ZD, Schmuki P (2011) Highly uniform Pt nanoparticle decoration on TiO_2 nanotube arrays: a refreshable platform for methanol electrooxidation. Electrochem Commun 13:290–293
61. Macak JM, Schmidt-Stein F, Schmuki P (2007) Efficient oxygen reduction on layers of ordered TiO_2 nanotubes loaded with Au nanoparticles. Electrochem Commun 9:1783–1787
62. Xiao F (2012) Layer-by-layer self-assembly construction of highly ordered metal-TiO_2 nanotube arrays heterostructures (M/TNTs, M = Au, Ag, Pt) with tunable catalytic activities. J Phys Chem C 116:16487–16498
63. Xiao F (2012) An efficient layer-by-layer self-assembly of metal-TiO_2 nanoring/nanotube heterostructures, M/T-NRNT (M = Au, Ag, Pt), for versatile catalytic applications. Chem Commun 48:6538–6540
64. Xiao F-X (2012) A novel route for self-assembly of gold nanoparticle-TiO_2 nanotube array (Au/TNTs) heterostructure for versatile catalytic applications: pinpoint position via hierarchically dendritic ligand. RSC Adv 2:12699–12701
65. Clavero C (2014) Plasmon-induced hot-electron generation at nanoparticle/metal-oxide interfaces for photovoltaic and photocatalytic devices. Nat Photonics 8:95–103
66. Yu J, Dai G, Huang B (2009) Fabrication and characterization of visible-light-driven plasmonic photocatalyst Ag/AgCl/TiO_2 nanotube arrays. J Phys Chem C 113:16394–16401
67. Wu F, Hu X, Fan J et al (2013) Photocatalytic activity of Ag/TiO_2 nanotube arrays enhanced by surface plasmon resonance and application in hydrogen evolution by water splitting. Plasmonics 2013(8):501–508
68. Xiao F-X, Hung S-F, Miao J et al (2014) Metal-cluster decorated TiO_2 nanotube arrays: a composite heterostructure toward versatile photocatalytic and photoelectrochemical applications. Small 11:554–567
69. Ghicov A, Macak JM, Tsuchiya H et al (2006) Ion implantation and annealing for an efficient N-doping of TiO_2 nanotubes. Nano Lett 6:1080–1082
70. Jiang Y, Wu M, Wu X et al (2009) Low-temperature hydrothermal synthesis of flower-like ZnO microstructure and nanorod array on nanoporous TiO_2 film. Mater Lett 63:275–278
71. Liu Z, Zhang X, Nishimoto S et al (2008) Highly ordered TiO_2 nanotube arrays with controllable length for photoelectrocatalytic degradation of phenol. J Phys Chem C 112:253–259
72. Kostedt WL, Ismail AA, Mazyck DW (2008) Impact of heat treatment and composition of ZnO-TiO_2 nanoparticles for photocatalytic oxidation of an azo dye. Ind Eng Chem Res 47:1483–1487

73. Liao DL, Badour CA, Liao BQ (2008) Preparation of nanosized TiO_2/ZnO composite catalyst and its photocatalytic activity for degradation of methyl orange. J Photochem Photobiol A Chem 194:11–19
74. Yu H, Zhang Z, Han M et al (2005) A general low-temperature route for large-scale fabrication of highly oriented ZnO nanorod/nanotube arrays. J Am Chem Soc 127:2378–2379
75. Yu QJ, Fu WY, Yu CL et al (2007) Fabrication and optical properties of large-scale ZnO nanotube bundles via a simple solution route. J Phys Chem C 111:17521–17526
76. Qiu J, Jin Z, Liu Z et al (2007) Fabrication of TiO_2 nanotube film by well-aligned ZnO nanorod array film and sol–gel process. Thin Solid Films 515:2897–2902
77. Qiu J, Yu W, Gao X, Li X (2006) Sol–gel assisted ZnO nanorod array template to synthesize TiO_2 nanotube arrays. Nanotechnology 17:4695–4698
78. Thitima R, Takashi S, Susumu Y (2008) Photovoltaic performance of hybrid solar cell with TiO_2 nanotubes arrays fabricated through liquid deposition using ZnO template. Sol Energy Mater Sol Cells 92:1445–1449
79. Kim SS, Na SI, Nah YC (2011) TiO_2 nanotubes decorated with ZnO rod-like nanostructures for efficient dye-sensitized solar cells. Electrochim Acta 58:503–509
80. Benkara S, Zerkout S (2010) Preparation and characterization of ZnO nanorods grown into aligned TiO_2 nanotube array. J Mater Environ Sci 1:173–188
81. Zhang Z, Yuan Y, Liang L et al (2008) Preparation and photoelectrocatalytic activity of ZnO nanorods embedded in highly ordered TiO_2 nanotube arrays electrode for azo dye degradation. J Hazard Mater 158:517–526
82. Yang HY, Yu SF, Lau SP et al (2009) Direct growth of ZnO nanocrystals onto the surface of porous TiO_2 nanotube arrays for highly efficient and recyclable photocatalysts. Small 5:2260–2264
83. Xiao F (2012) Construction of highly ordered ZnO–TiO_2 nanotube arrays (ZnO/TNTs) heterostructure forphotocatalytic application. ACS Appl Mater Interface 4:7055–7063
84. Xiao F-X, Hung S-F, Tao HB et al (2014) Spatially branched hierarchical ZnO nanorod-TiO_2 nanotube array heterostructures for versatile photocatalytic and photoelectrocatalytic applications: towards intimate integration of 1D-1D hybrid nanostructures. Nanoscale 6:14950–14961
85. Xiao F-X, Miao J, Wang H-Y et al (2014) Electrochemical construction of hierarchically ordered CdSe-sensitized TiO_2 nanotube arrays: towards versatile photoelectrochemical water splitting and photoredox applications. Nanoscale 6:6727–6737
86. Xiao F-X, Miao J, Wang H-Y et al (2013) Self-assembly of hierarchically ordered CdS quantum dots-sensitized TiO2 nanotube array heterostructure as efficient visible light photocatalyst for photoredox applications. J Mater Chem A 1:12229–12238
87. Zhang Y, Tang Z-R, Fu X et al (2011) Self-assembly of hierarchically ordered CdS quantum dots–TiO_2 nanotube array heterostructures as efficient visible light photocatalysts for photoredox applications. Appl Catal B 106:445–452
88. Zhang N, Ciriminna R, Pagliaro M et al (2014) Nanochemistry-derived Bi_2WO_6 nanostructures: Towards production of sustainable chemicals and fuels induced by visible light. Chem Soc Rev 43:5276–5287
89. Weng B, Liu S, Tang Z-R et al (2014) One-dimensional nanostructure based materials for versatile photocatalytic applications. RSC Adv 4:12685–12700
90. Fujishima A, Rao TN, Tryk DA (2000) Titanium dioxide photocatalysis. J Photochem Photobiol C 1:1–21
91. Xiao F (2012) Self-assembly preparation of gold nanoparticles-TiO_2 nanotube arrays binary hybrid nanocomposites for photocatalytic applications. J Mater Chem 22:7819–7830
92. Zhang X, Han F, Shi B et al (2012) Photocatalytic conversion of diluted CO_2 into light hydrocarbons using periodically modulated multiwalled nanotube arrays. Angew Chem Int Ed 51:12732–12735

93. Li X, Liu H, Luo D et al (2012) Adsorption of CO_2 on heterostructure $CdS(Bi_2S_3)/TiO_2$ nanotube photocatalysts and their photocatalytic activities in the reduction of CO_2 to methanol under visible light irradiation. Chem Eng J 180:151–158
94. Feng X, Sloppy JD, LaTempa TJ et al (2011) Synthesis and deposition of ultrafine Pt nanoparticles within high aspect ratio TiO_2 nanotube arrays: application to the photocatalytic reduction of carbon dioxide. J Mater Chem 21:13429–13433
95. Varghese OK, Paulose M, LaTempa TJ et al (2009) High-rate solar photocatalytic conversion of CO_2 and water vapor to hydrocarbon fuels. Nano Lett 9:731–737
96. Roy SC, Varghese OK, Paulose M et al (2010) Toward solar fuels: photocatalytic conversion of carbon dioxide to hydrocarbons. ACS Nano 4:1259–1278
97. Beranek R, Tsuchiya H, Sugishima T et al (2005) Enhancement and limits of the photoelectrochemical response from anodic TiO_2 nanotubes. Appl Phys Lett 87:243114–243116
98. Roy P, Berger S, Schmuki P (2011) TiO_2 nanotubes: synthesis and applications. Angew Chem Int Ed 50:2904–2939
99. Zhang Z, Zhang L, Hedhili MN et al (2013) Plasmonic gold nanocrystals coupled with photonic crystal seamlessly on TiO_2 nanotube photoelectrodes for efficient visible light photoelectrochemical water splitting. Nano Lett 13:14–20. http://pubs.acs.org/doi/abs/10.1021/nl3029202
100. Ye M, Gong J, Lai Y et al (2012) High-efficiency photoelectrocatalytic hydrogen generation enabled by palladium quantum dots-sensitized TiO_2 nanotube arrays. J Am Chem Soc 134:15720–15723
101. Allam NK, Poncheri AJ, EI-Sayed MA et al (2011) Vertically oriented Ti–Pd mixed oxynitride nanotube arrays for enhanced photoelectrochemical water splitting. ACS Nano 5:5056–5066
102. Mor GK, Prakasam HE, Varghese OK et al (2007) Vertically oriented Ti-Fe-O nanotube array films: toward a useful material architecture for solar spectrum water photoelectrolysis. Nano Lett 7:2356–2364
103. Allam NK, Alamgir F, EI-Sayed MA (2010) Enhanced photoassisted water electrolysis using vertically oriented anodically fabricated Ti−Nb−Zr−O mixed oxide nanotube arrays. ACS Nano 4:5819–5826
104. Feng X, LaTempa T, Basham JI et al (2010) Ta_3N_5 nanotube arrays for visible light water photoelectrolysis. Nano Lett 2010(10):948–952